The Construction and Exploration of the ceRNA Network and Patterns of Tumor-Infiltrating Immune Cells in Kidney Renal Clear Cell Carcinoma

Weiwei Jia
Basic Medical Sciences Center, Shanxi Medical University, Taiyuan, PR China. Department of Pathology, Shanxi Medical University, Taiyuan, PR China

Pengjia Li
Basic Medical Sciences Center, Shanxi Medical University, Taiyuan, PR China. Department of Pathology, Shanxi Medical University, Taiyuan, PR China

Mingxia Ma
Basic Medical Sciences Center, Shanxi Medical University, Taiyuan, PR China. Department of Pathology, Shanxi Medical University, Taiyuan, PR China

Xiaochen Niu
The Second Clinical College of Shanxi Medical University, Taiyuan, PR China

Lina Bai
Basic Medical Sciences Center, Shanxi Medical University, Taiyuan, PR China

Haihu Hao
Department of Orthopedics, Shanxi Bethune Hospital & Shanxi Academy of Medical Sciences, Taiyuan, PR China

Xiaohui Wang
Basic Medical Sciences Center, Shanxi Medical University, Taiyuan, PR China. Department of Pathology, Shanxi Medical University, Taiyuan, PR China

Li Wang (mirror0117@126.com)
Shanxi Medical University

Research

Keywords: KIRC, CeRNA network, Tumor-infiltrating immune cells, prognosis

Posted Date: November 25th, 2020

DOI: https://doi.org/10.21203/rs.3.rs-113464/v1

Abstract

Background: Kidney renal clear cell carcinoma is the malignant tumor with the highest incidence and poor prognosis in renal cell carcinoma. In view of its limited diagnostic strategies and poor prognosis, bioinformatics analysis has been used to explore the possible mechanisms of renal clear cell carcinoma and effective prognostic-related biomarkers.

Method: The sequencing information of 3 types of RNA (mRNA, lncRNA and miRNA) in 539 cases of kidney renal clear cell carcinoma tumor tissues and 72 cases of normal tissues is obtained from the TCGA database. Heat map and volcano map of differentially expressed genes were drawn through R language; The CeRNA network was visualized by Cytoscape software (version 3.7.2). Methods such as univariate Cox regression analysis, lasso regression screening, and multivariate Cox regression analysis were used to construct a prognostic model based on the CeRNA network. The CIBERSORT algorithm was used to analyze the degree of infiltration of 22 kinds of immune cells from each sample of kidney renal clear cell carcinoma. Construction of a prognostic model based on tumor-infiltrating immune cells, The R "corrplot" software package was used for co-expression analysis based on the CeRNA network and tumor-infiltrating immune cells model.

Results: There are 3074 differentially expressed mRNAs (1055 upregulated and 2019 downregulated), and 359 differentially expressed lncRNAs (71 upregulated and 280 downregulated) and 132 differentially expressed miRNAs (70 upregulated and 62 downregulated) that have been identified through differential analysis. A complete mRNA-miRNA-lncRNA (SIX1-hsa-miR-200b-3p-MALAT1) network was obtained based on the CeRNA network-based prognostic model construction. 2 immune cells (Mast cells resting, T cells follicular helper) were identified by constructing a prognostic model based on tumor-infiltrating immune cells. There was a negative correlation between lncRNA MALAT1 and Mast cells resting ($R=-0.27$, $P<0.001$); while there was a positive correlation between lncRNA MALAT1 and T cells follicular helper ($R=0.23$, $P<0.001$).

Conclusion: Based on CeRNA network and tumor-infiltrating immune cells, we explored the possible mechanism of kidney renal clear cell carcinoma and obtained effective biomarkers for predicting prognosis by Bioinformatics analysis in this study.

Background

Renal cell carcinoma (RCC) is one of the top ten malignant tumors in the world [1]. Compared with other subtypes of RCC, kidney renal clear cell carcinoma (KIRC) is the most common histopathological type and has a poor prognosis [2]. Many patients have progressed to the advanced stage when they are diagnosed, and the 5-year survival rate (FSR) has also decreased significantly, because the early clinical symptoms and signs of KIRC are relatively insidious and non-specific [3]. In view of the limited diagnostic strategies and poor prognosis of KIRC, we urgently need to search for biological markers which are helpful for diagnosis, targeted therapy and prognosis prediction.

Messenger RNA (mRNA) is a protein coding gene, which participates in the formation and development of KIRC. Recently, non coding RNA had also drawn remarkable attention, particularly in terms of microRNA (miRNA) and long non coding RNA (lncRNA), which is indispensable for the regulation of cellular processes [4]. The competitive endogenous RNA (CeRNA) hypothesis is that lncRNA could compete for the miRNA recognizing elements (MRE) to influences the mRNA regulation, and which is put forward by Salmena et al. Recent studies have shown that CeRNA networks control biological behaviors, which via regulating oncogenes and tumor suppressor genes, such as tumor invasion and metastasis [5]. However, there is no definition of CeRNA network to predict the prognosis of KIRC. Therefore, in this study, we constructed a CeRNA network about KIRC to identify the potential interactions involved in the differentially expressed lncRNA, miRNA and mRNA in KIRC, which to determine the molecular targets of prognostic evaluation.

Surgical treatment is the only effective treatment method for localised KIRC, but patients with metastatic must be treated with systemic therapy [6]. However, due to the long-term use of systemic therapy and the development of tumors, the occurrence of tumor immune escape has been promoted [2]. Some immunosuppressive factors may be hijacked by cancer cells to avoid the attack of immune system [7]. It is essential to maintain the host's immune homeostasis and eliminate cancer cells by balancing immune stimulus factors and inhibitory factors [8]. Recent studies have shown that immunotherapy has become an important method to improve the survival rate of patients with KIRC [9]. Recently, a number of evidences show that miRNA can regulate cancer immune surveillance and promote immune escape [10]. It is not clear how miRNA (as the regulatory hub of CeRNA) changes the CeRNA network and how CeRNA changes the immune cells of KIRC, and the correlation between the two changes.

We use bioinformatics analysis to construct a complete gene interaction CeRNA network. By screening the differentially expressed lncRNA, miRNA and mRNA in KIRC, in order to explore the key genes involved in the development of KIRC. We conducted co-expression analysis based on the risk genes related to prognosis and the differentially expressed immune cells in KIRC to further explore the potential molecular mechanism of KIRC. Not only that, we further explored the relationship between CeRNA and immune infiltration, and finally obtained the connection between CeRNA network and immune cells. Our researchs provide new insights into the occurrence and development of KIRC, as well as survival prediction biomarkers and potential therapeutic targets.

Methods

1.1 Data download and differential gene expression analysis

There are 539 KIRC and 72 normal tissues of 3 types of RNA information (including mRNA, lncRNA and miRNA) and the clinical data were downloaded by using the GDC RNA toolkit package of the R language (R 4.0.2) in the cancer genome atlas database[43]. Firstly, We used the log(fold change，FC)≥1 or ≤1 and false discovery rate (FDR) adjusted P value<0.05 as criteria to identify significant differential genes. The heat maps were drawn by the "pheatmap" R package, and the volcano maps were drawn by the "ggplot2"

R package. Then, hypergeometric testing and correlation analysis were used to select significantly different and related genes, and use Cytoscape v.3.7.2 software to visualize the CeRNA network. It does not require relevant ethical review and approval, due to the data used in this study came from the TCGA database.

1.2 Construction of prognosis model related to CeRNA network

The expression levels of nodes in CeRNA network were combined with clinical data by using perl (perl 5.26.3) language. The network nodes related to survival prognosis were selected by Kaplan-Meier survival analysis using the R "survival" package according to the filter condition: P <0.05. The construction of the prognostic model based on the CeRNA network was completed by single factor Cox regression analysis, lasso regression and multivariate Cox regression analysis. The formula of prognosis model: risk score= expression of risk genes$_1$*coef$_1$+expression of risk genes$_2$*coef$_2$+...expression of risk genes$_n$ * coef$_n$. The survival curve of the model and the time-dependent receiver operating characteristic curve (ROC) were drawn, in order to estimate the accuracy and resolution of the model.

1.3 CIBERSORT algorithm Evaluation

The CIBERSORT algorithm was used to estimate the degree of infiltration of 22 immune cell types in each KIRC sample, with a CIBERSORT output of p <0.05, indicated that the Example of these cells were significant, which was worthy of further study. We evaluated the difference between immune infiltrating cells in tumor tissue and normal tissue with Wilcoxon rank-sum test. Finally, histogram and differential heat map of tumor-infiltrating immune cells were drawn.

1.4 Construction of immune infiltration model

The degree of tumor-infiltrating immune cells in each tumor sample was combined with clinical information to evaluate the prognostic value of immune cell infiltration in tumor tissues, and then the survival curve was drawn by Kaplan-Meier survival analysis using the survival package (P<0.05). The prognosis model based on the degree of tumor-infiltrating immune cells in each sample was combined with clinical information to evaluate the prognostic value of immune cell infiltration in tumor tissues, and then the survival curve was drawn by Kaplan-Meier survival analysis using the survival package was constructed by single factor Cox regression analysis, lasso regression and multivariate Cox regression analysis. The survival curve of the model and the ROC curve of the model were drawn.

1.5 Co-expression analysis

In order to evaluate the co-expression of the key tumor-infiltrating immune cells and key nodes in the CeRNA network, and to explore the correlation between tumor-infiltrating immune cells and CeRNA network expression, the "Corrplot" R package was used to perform co-expression analysis on the key nodes based on the CeRNA network and the key cells based on the tumor-infiltrating immune cells model,

and output significant related pairs. According to the correlation analysis, the corrected P value was 0.001.

Results

2.1 The Flow chart of the Analytical Process

2.2 Identification of Differentially expressed Genes

The RNA-sequencing information was downloaded in 539 tumor tissues and 72 normal tissue samples from TCGA-KIRC database. There were 3074 differentially expressed mRNAs (1055 upregulated and 2019 downregulated, Figure 2a, d), and 359 differentially expressed lncRNAs (71 upregulated and 280 downregulated, Figure 2b, e) and 132 differentially expressed miRNAs (70 upregulated and 62 downregulated, Figure 2c, f). The difference information was shown in supplementary table 1-3.

2.3 Construction of CeRNA Network

20 mRNAs, 7 lncRNAs and 14 miRNAs with significant differences were obtained through the analysis of hypergeometric distribution test and correlation test (P<0.001) . In this study, we constructed a CeRNA network using these significantly different RNAs (Figure 3), and the detail information was shown in supplementary table 4.

2.4 Construction of Risk Prognosis Model

9 risk genes were obtained through lasso regression analysis (Figure 4a, 4b) and multi-factor COX regression analysis (Figure 4e)，including 5 mRNAs (RELT, MYO9B, KCNN, SIX1, OTOGL), 1 lncRNA (MALAT1) and 3 miRNAs (hsa-miR-130b-3p, hsa-miR-200b-3p, hsa-miR-21-5p). And the risk score (RS) of the risk prognosis model according to this formula (RS=RELT*0.228-MYO9B*0.546+KCNN4*0.265+SIX1*0.135-OTOGL*0.142+MALAT1*0.223+hsa-miR-130b-3p*0.321-hsa-miR-200b-3p*0.091+hsa-miR-21-5p*0.254) was calculated. After matched the risk genes to the CeRNA network, we obtained a complete mRNA-miRNA-lncRNA (SIE1-hsa-miR-200b-3p-MALAT1) relationship chain. The survival curve of the model was drawn by the Kaplan-Meier method. The results showed that the survival rate of patients in the high-risk group was significantly lower than that of the low-risk group (Figure 4c). In order to estimate the accuracy of the model, we have further drawn the ROC curve (1-year AUC: 0.769; 3-year AUC: 0.750; 5-year AUC: 0,771, Figure 4d).

2.5 Evaluation of CIBERSORT algorithm and Construction of Immune Infiltration Model

The proportions of 22 immune cells in different samples were provided by CIBERSORT algorithm analysis (Figures 5a, 5b). 2 tumor-infiltratings immune cells (Mast cells resting, T cells follicular helper) were identified by lasso regression analysis (Figure 6a, 6b) and multivariate Cox regression analysis (Figure 6e). The formula for the constructed prognosis model related to immune infiltration was: risk score=T cells follicular helper*10.132-Mast cells resting*10.401. The survival curve of the model was drawn by the

Kaplan–Meier method. The results showed that the survival rate of patients in the high-risk group was significantly lower than that in the low-risk group (Figure 6c). We further drawn the ROC curve to estimate the accuracy of the model (1-year AUC: 0.589; 3-year AUC: 0.633; 5-year AUC: 0,610, Figure 6d).

2.6 The Correlation Analysis of Risk Immune Cells and Clinical

Firstly, the R language was used to draw a heat map of the differential expression of risk immune cells in the low-risk group and the high-risk group. The results showed that as the risk score increased, the cell content of T cells follicular helper gradually increased , while the cell content of Mast cells resting gradually decreased (Figure 7a). Then we also analyzed the proportions of two different subtypes of immune cells in different clinical staging using non-parameter test and Kaplan-Meier method. The results demonstrated that the expression quantitative of T cells follicular helper in stage IV patients was significantly higher than in stage I patients (Figure 7b), and the expression quantitative of Mast cells resting decreased significantly as the stage level increased (Figure 7c).

2.7 Co-expression Analysis

The co-expression relationship graph was obtained by analyzing the correlation between the tumor-infiltrating immune cells model and the CeRNA network nodes by using Pearson correlation analysis (Figure 8a, b). There was a negative correlation between Mast cells resting and T cells follicular helper (R= -0.26, see Figure 8A, B), lncRNA MALAT1 and Mast cells resting was negative correlation. (R= -0.27, P<0.001, Figure 8c), however there was a positive association of lncRNA MALAT1 with T cells follicular helper (R=0.23, P<0.001, Figure 8d). And the detail information was shown in supplementary table 5.

Discussion

Renal cell carcinoma is one of the most deadly cancers in the urinary system, and its incidence is increasing year by year [11]. KIRC accounts for about 80% of all RCC histological subtypes and had the high mortality, invasiveness and metastasis rate [12]. Characteristic changes at the molecular level play a crucial role in the occurrence and metastasis of tumors, and had been considered as prognostic factors [13]. We found that the genes and tumor-infiltrating immune cells are differentially expressed between KIRC tumor tissue and normal tissue. In response to this finding, we constructed risk prediction models based on CeRNA network and tumor-infiltrating immune cells. Among them, we analyzed the correlation between CeRNA network and tumor-infiltrating immune cells, we inferred a potential mechanism of KIRC recurrence and that was lncRNA MALTA1 regulating Mast cells resting (MCs) and T cells follicular helper (TFH). Our findings could help clinical oncologists assess the prognosis and risk of recurrence of KIRC.

CeRNA network is that lncRNA compete for the miRNA recognition elements (MRE) to influences the mRNA regulation, thus, we speculate that this type of analysis could uncover molecular interactions and gene regulatory networks that have been missed by proteomic and conventional genomic methods [5]. Studies shown that 3’UTRs from coding genes may act as endogenous decoys, which binds to the MRE recognition sequence of miRNA through the principle of complementary base pairing and participates in

post-transcriptional regulation of oncogenes and tumor suppressors [14], and lncRNA can also competitively bind the MRE sequence of miRNA to regulate the expression level of mRNA in tumor cells [15]. More importantly, lncRNA modulated mitochondrial membrane potential and enhanced the release of cytochrome C, indicating that apoptosis of KIRC induced by lncRNA may belong to mitochondria-mediated apoptosis [16], and lncRNA can also participate in the proliferation of cancer cells by promoting the expression level of KIRC distant metastasis related genes[17]. In this study, we obtain 3074 differentially expressed mRNA (1055 upregulated and 2019 downregulated), 359 differentially expressed lncRNA (71 upregulated and 280 downregulated), and 132 differentially expressed miRNA(70 upregulated and 62 downregulated) through bioinformatics analysis the RNA sequencing (RNA-seq) data of KIRC. We have constructed a CeRNA network that can prepare the prognosis of KIRC through the analysis of hypergeometric distribution test and correlation test, which contains 20 mRNAs, 7 lncRNAs and 14 miRNAs. And then ,we use the single factor COX analysis, lasso regression and multivariate Cox regression analysis to obtain 9 genes (RELT, MYO9B, KCNN4, SIX1, OTOGL, MALAT1, HSA-Mir-130b-3P, HSA-Mir-200b-3p, HSA-Mir-21-5p) in CeRNA that were significantly correlated with the overall survival rate of KIRC. We constructed a prognostic model using these risk genes and got the AUC values (for 1-year survival rates: 0.794, 3-year survival rates: 0.762, and 5-year survival rates: 0.782). After matching the 9 risk genes and the CeRNA network, it was found that hsa-miR-200-3p (miRNA), SIX1 (mRNA) and MALAT1 (lncRNA) were significantly correlated (P = 4.30E-6). SIX1 is a key transcription factor involved in the occurrence and development of a lot of tumor and its biological activity is regulated by miRNA [18, 19]. SIX1 may contribute to ovarian epithelial carcinogenesis by simultaneously increasing proliferation and decreasing apoptosis and imply that SIX1 may be an important target of ovarian cancer therapy response [19]. SIX1 can regulate the mitochondrial membrane potential by regulating the expression of the anti-apoptotic protein Bcl-2, and affect mitochondrial apoptosis via caspase-7, which suggests that SIX1 can be used as an effective target for the prognosis and treatment of gastric cancer [20]. However, there is few study had clearly shown the relationship between SIX1 and KIRC. Our results show that the decreased expression of miR-200 in KIRC may be involved in the formation and development of cancer by promoting the increased expression of SIX1.

Many previous studies have shown that the miR-200 family members of KIRC were significantly downregulated compared with normal kidney tissue. It is speculated that miR-200b as tumor biomarkers in renal tumor biopsies is feasible [21, 22]. Rola Saleeb et al. found that miR-200b was down-regulated in primary KIRC and further decreased in metastatic foci. More importantly, Kaplan-Meier survival curves indicate that miR-200b and miR-200c positive patients have significantly longer disease-free survival [23]. Therefore, the expression of miR-200 is negatively correlated with the progression of KIRC. In this study, we found that the HR value of miR-200 was less than 1 through single-factor COX, lasso regression and multi-factor COX analysis, indicating that miR-200 is a gene that protects renal clear cell carcinoma. This is consistent with the results of miR-200 family members mentioned in previous studies that inhibit the proliferation, migration, and invasion of cancer cells [24].

There is another important RNA in the significantly related network of hsa-miR-200-3p(miRNA)-SIX1(mRNA)-MALAT1(lncRNA), this is lncRNA MALAT1. Metastasis associated with lung

adenocarcinoma transcript-1 (MALAT1) is one of the long non-coding RNA (lncRNA) associated with tumors which is composed of more than 8000 nucleotides and located on chromosome 11q13 [25]. MALAT1 was initially considered to be an effective prognostic factor for non-small cell lung cancer (NSCLC), tumors with high MALAT1 expression have a nearly five-fold increase in the risk of metastasis compared with tumors with low MALAT-1 expression [26]. Feng et al. proved that the direct binding between MALAT1 and miR-200a can promote the proliferation of lung cancer cells and lead to the development of gefitinib resistance [27]. In addition to NSCLC, MALAT1 is also present in other malignant tumors. In endometrial cancer, the expression of MALAT1 is negatively correlated with the expression of miR-200c, and its knockdown can promote the expression of miR-200c in cancer cells [28]. Studies have found that MALAT1 can also adjust the expression of miR-140 in prostate cancer cells to change the mRNA and protein expression levels of apoptosis inhibitor protein to promote the occurrence and development of tumors [29]. More importantly, some studies have shown that MALAT1 in KIRC promotes the growth of cancer cells by inhibiting cell apoptosis and accelerating the expression of specific proteins of epithelial-mesenchymal transition (EMT) [30]. In this study, we found that MALAT1 is a high-risk factor in KIRC through bioinformatics analysis, and its expression level is positively correlated with tumor formation and development, which is consistent with the role of MALAT1 in other tumors. Therefore, we speculate that hsa-miR-200-3p (miRNA) - SIX1 (mRNA) - MALAT1 (lncRNA) plays an important role in the development of renal clear cell carcinoma. However, how these genes affect the occurrence and development of KIRC is still unclear.

In the past few decades, more and more evidences show that the tumor-cell phenotype is determined by the intrinsic activity of cancer cells and the interaction of cells (especially tumor-infiltrating immune cells, TIICs) in the tumor microenvironment [31, 32]. Complex interactions between the immune cells in this microenvironment may promote cancer progression by inducing immune dysfunction in RCC patients [33]. Interestingly, lncRNA MALAT1 is an important inflammation regulator. In patients with systemic lupus erythematosus (SLE), lncRNA MALAT1 can be used as a CeRNA to interfere with the inhibitory effect of miRNA on the inflammatory factor IL-21, so the expression of MALAT1 in SLE patients is significantly increased [34]. During an asthma attack, MALAT1 activates airway inflammation and airway hyperresponsiveness of T cells by inducing the expression of miR-155 in T cells [35, 36]. However, it is not clear whether lncRNA MALAT1 is involved in the process of immune invasion, immune cell killing and immune escape in the tumor microenvironment of RCC.

In this study, we analyzed the correlation between gene expression and tumor-infiltrating immune cells to prove that MALAT1 and MCs, (R = -0.27, P = 8.95E-5), MALAT1 and TFH (R = 0.23, P = 9.85E-4) were significantly correlated. Therefore, Therefor, we speculate that MALAT1, the core molecule of the CeRNA network, participates in the occurrence of KIRC by regulating the content of tumor-infiltrating immune cells, such as TFH and MCs.

We first analyzed by using the CIBERSORT algorithm and found that the expression levels of resting MCs and TFH between KIRC and normal tissues are significantly different. Compared with other algorithms, CIBERSORT is the best algorithm to distinguish between resting and IgE-activated MCs. Our results

suggested that most of the MCs in KIRC are in resting state. Studies have shown that MCs activated by IgE can prevent the occurrence of cancer [37]. However, there are high concentrations of polyamines in malignant tumor cells [38]. Polyamines oxidized by polyamine oxidase can prevent the activation of MCs by IgE, thereby inhibiting the tumor suppressor effect of resting MCs [39]. The resting MCs in KIRC can promote the immune escape of tumor cells, which is beneficial to tumors growth [40]. Therefore, when the content of resting MC is higher, it may promote the occurrence of tumors. We observed that the expression of MALAT1 increased in KIRC tumor tissues, and the content of resting MCs decreased observably. There is a negative correlation between MALAT1 and MCs. Above all, we speculate that MALAT1 may affect the generation of KIRC by the content of resting MCs.

TFH is an immune cell located in the peritumoral tertiary lymphoid structures (TLS), which belongs to a subset of $CD4^+$ T cells [41]. TFH provides signals for the proliferation and activation of B cells by secretes a large number of chemokines in B cell [42]. Our results proved that the expression of lncRNA MALAT1 in the CeRNA network is positively correlated with the contents of TFH. The expression of MALAT1 in KIRC cells is increased, which suggested that the content of TFH in KIRC cells is higher than that in normal tissues. By using Multi-factor COX analysis, we found that the content of TFH in KIRC cells is ascended distinctly, which is consistent with our speculation. Therefore, we believed that TFH may be one of the maker cells of immune infiltration in KIRC.

In summary, this study constructed a KIRC related CeRNA network through the TCGA database, and selected risk genes through single factor COX analysis, lasso regression and multivariate Cox regression analysis to predict the survival rate of patients. We obtained a significant correlation network of hsa-miR-200-3p(miRNA)-SIX1(mRNA)-MALAT1(lncRNA) through correlation analysis. In order to explore how the genes in this network affect the formation of KIRC, this study also constructed another risk model based on tumor-infiltrating immune cells, and screened out risky tumor-infiltrating immune cells related to the occurrence and development of KIRC. We speculated that hsa-miR-200-3p and MALAT1 affect the internal mechanism of KIRC by regulating the expression of SIX1, and the relationship between MALAT1 and immune infiltration, so as to promote the self-management of KIRC patients.

Our research is a correlation study from multiple dimensions rather than a biological mechanism study. Based on the results of this research, we will verify our conclusions through biological experiments. In the future, we will combine more data and more experiments to explore the impact of KIRC molecular biology on CeRNA, as well as the relationship between tumor cells, TFH and resting MCs.

Conclusion

Based on the bioinformatics analysis of the CeRNA network and tumor-infiltrating immune cells, our research inferred that hsa-miR-200-3p, MALAT1 and SIX1 are involved in the internal mechanism of KIRC, and the relationship between MALAT1 and tumor-infiltrating immune cells (MCs, TFH)

Abbreviations

RCC: Renal Cell Carcinoma

KIRC: Kidney Renal Clear Cell Carcinoma

CeRNA: Competing Endogenous RNA

MCs: Mast Cells resting

TFH: T cells Follicular Helper

mRNA: Messenger RNA

lncRNA: Long Non-Coding RNA

miRNA: MicroRNA

MRE: MiRNA Recognition Elements

NSCLC: Non-Small Cell Lung Cancer

RNA-seq: RNA Sequencing

TIICs: Especially Tumor-Infiltrating Immune Cells,

SLE: Systemic Lupus Erythematosus

TLS: Tertiary Lymphoid Structures

FSR: 5-year Survival Rate

FC: Fold Change

FDR: False Discovery Rate

ROC: Receiver Operating Characteristic

Declarations

Acknowledgements

Not applicable

Authors' contributions

WW Jia analyzed and explained the RNA-seq and clinical data of TCGA-KIRC, and was the main contributor to the manuscript. L Wang directed the writing of the manuscript. XH Wang directed the writing of the manuscript. The final manuscript read and approved by all authors.

Funding

This work was sponsored by the Fund for Shanxi “1331 Project” Key Subjects Construction.

Ethics approval and consent to participate

Not applicable.

Consent for publication

All authors reviewed and approved the final version for submission.

Availability of data and material

The data set used in this study is a publicly available data set. This data can be found here: TCGA (https://tcga-data.nci.nih.gov/tcga/).

Competing interests

The authors declare that they have no competing interests.

References

1. Siegel RL, Miller KD, Jemal A: **Cancer statistics, 2018**. *CA Cancer J Clin* 2018, **68**(1):7-30.
2. Xiao GF, Yan X, Chen Z, Zhang RJ, Liu TZ, Hu WL: **Identification of a Novel Immune-Related Prognostic Biomarker and Small-Molecule Drugs in Clear Cell Renal Cell Carcinoma (ccRCC) by a Merged Microarray-Acquired Dataset and TCGA Database**. *Front Genet* 2020, **11**:810.
3. Gupta K, Miller JD, Li JZ, Russell MW, Charbonneau C: **Epidemiologic and socioeconomic burden of metastatic renal cell carcinoma (mRCC): a literature review**. *Cancer Treat Rev* 2008, **34**(3):193-205.
4. Yan Y, Xu Z, Li Z, Sun L, Gong Z: **An Insight into the Increasing Role of LncRNAs in the Pathogenesis of Gliomas**. *Front Mol Neurosci* 2017, **10**:53.
5. Salmena L, Poliseno L, Tay Y, Kats L, Pandolfi PP: **A ceRNA hypothesis: the Rosetta Stone of a hidden RNA language?** *Cell* 2011, **146**(3):353-358.
6. Ljungberg B, Bensalah K, Canfield S, Dabestani S, Hofmann F, Hora M, Kuczyk MA, Lam T, Marconi L, Merseburger AS *et al*: **EAU guidelines on renal cell carcinoma: 2014 update**. *Eur Urol* 2015, **67**(5):913-924.
7. Yi M, Xu L, Jiao Y, Luo S, Li A, Wu K: **The role of cancer-derived microRNAs in cancer immune escape**. *J Hematol Oncol* 2020, **13**(1):25.
8. Alissafi T, Hatzioannou A, Legaki AI, Varveri A, Verginis P: **Balancing cancer immunotherapy and immune-related adverse events: The emerging role of regulatory T cells**. *J Autoimmun* 2019, **104**:102310.

9. Coppin C, Porzsolt F, Awa A, Kumpf J, Coldman A, Wilt T: **Immunotherapy for advanced renal cell cancer**. *Cochrane Database Syst Rev* 2005(1):CD001425.
10. Omar HA, El-Serafi AT, Hersi F, Arafa EA, Zaher DM, Madkour M, Arab HH, Tolba MF: **Immunomodulatory MicroRNAs in cancer: targeting immune checkpoints and the tumor microenvironment**. *FEBS J* 2019, **286**(18):3540-3557.
11. Siegel RL, Miller KD, Jemal A: **Cancer statistics, 2019**. *CA Cancer J Clin* 2019, **69**(1):7-34.
12. Xiao W, Wang X, Wang T, Xing J: **Overexpression of BMP1 reflects poor prognosis in clear cell renal cell carcinoma**. *Cancer Gene Ther* 2020, **27**(5):330-340.
13. Rodina A, Wang T, Yan P, Gomes ED, Dunphy MP, Pillarsetty N, Koren J, Gerecitano JF, Taldone T, Zong H *et al*: **The epichaperome is an integrated chaperome network that facilitates tumour survival**. *Nature* 2016, **538**(7625):397-401.
14. Ye Z, Duan J, Wang L, Ji Y, Qiao B: **LncRNA-LET inhibits cell growth of clear cell renal cell carcinoma by regulating miR-373-3p**. *Cancer Cell Int* 2019, **19**:311.
15. Yi N, Liao QP, Li ZH, Xie BJ, Hu YH, Yi W, Liu M: **RNA interference-mediated targeting of DKK1 gene expression in Ishikawa endometrial carcinoma cells causes increased tumor cell invasion and migration**. *Oncol Lett* 2013, **6**(3):756-762.
16. Rupaimoole R, Slack FJ: **MicroRNA therapeutics: towards a new era for the management of cancer and other diseases**. *Nat Rev Drug Discov* 2017, **16**(3):203-222.
17. Zheng S, Jiang F, Ge D, Tang J, Chen H, Yang J, Yao Y, Yan J, Qiu J, Yin Z *et al*: **LncRNA SNHG3/miRNA-151a-3p/RAB22A axis regulates invasion and migration of osteosarcoma**. *Biomed Pharmacother* 2019, **112**:108695.
18. Yang X, Zhu X, Yan Z, Li C, Zhao H, Ma L, Zhang D, Liu J, Liu Z, Du N *et al*: **miR-489-3p/SIX1 Axis Regulates Melanoma Proliferation and Glycolytic Potential**. *Mol Ther Oncolytics* 2020, **16**:30-40.
19. Behbakht K, Qamar L, Aldridge CS, Coletta RD, Davidson SA, Thorburn A, Ford HL: **Six1 overexpression in ovarian carcinoma causes resistance to TRAIL-mediated apoptosis and is associated with poor survival**. *Cancer Res* 2007, **67**(7):3036-3042.
20. Du P, Zhao J, Wang J, Liu Y, Ren H, Patel R, Hu C, Zhang W, Huang G: **Sine Oculis Homeobox Homolog 1 Regulates Mitochondrial Apoptosis Pathway Via Caspase-7 In Gastric Cancer Cells**. *J Cancer* 2017, **8**(4):636-645.
21. Silva-Santos RM, Costa-Pinheiro P, Luis A, Antunes L, Lobo F, Oliveira J, Henrique R, Jeronimo C: **MicroRNA profile: a promising ancillary tool for accurate renal cell tumour diagnosis**. *Br J Cancer* 2013, **109**(10):2646-2653.
22. Akiya S, Nagaya K, Fukui A, Hamada T, Takahashi H, Furukawa H: **Inherited corneal amyloidosis predominantly manifested in one eye**. *Ophthalmologica* 1991, **203**(4):204-207.
23. Saleeb R, Kim SS, Ding Q, Scorilas A, Lin S, Khella HW, Boulos C, Ibrahim G, Yousef GM: **The miR-200 family as prognostic markers in clear cell renal cell carcinoma**. *Urol Oncol* 2019, **37**(12):955-963.

24. Chen X, Wang X, Ruan A, Han W, Zhao Y, Lu X, Xiao P, Shi H, Wang R, Chen L *et al*: **miR-141 is a key regulator of renal cell carcinoma proliferation and metastasis by controlling EphA2 expression**. *Clin Cancer Res* 2014, **20**(10):2617-2630.
25. Ji P, Diederichs S, Wang W, Boing S, Metzger R, Schneider PM, Tidow N, Brandt B, Buerger H, Bulk E *et al*: **MALAT-1, a novel noncoding RNA, and thymosin beta4 predict metastasis and survival in early-stage non-small cell lung cancer**. *Oncogene* 2003, **22**(39):8031-8041.
26. Gutschner T, Hammerle M, Diederichs S: **MALAT1 -- a paradigm for long noncoding RNA function in cancer**. *J Mol Med (Berl)* 2013, **91**(7):791-801.
27. Feng C, Zhao Y, Li Y, Zhang T, Ma Y, Liu Y: **LncRNA MALAT1 Promotes Lung Cancer Proliferation and Gefitinib Resistance by Acting as a miR-200a Sponge**. *Arch Bronconeumol* 2019, **55**(12):627-633.
28. Chen G, Zhang M, Liang Z, Chen S, Chen F, Zhu J, Zhao M, He J, Hua W, Duan P: **Association of polymorphisms in MALAT1 with the risk of endometrial cancer in Southern Chinese women**. *J Clin Lab Anal* 2020, **34**(4):e23146.
29. Hao T, Wang Z, Yang J, Zhang Y, Shang Y, Sun J: **MALAT1 knockdown inhibits prostate cancer progression by regulating miR-140/BIRC6 axis**. *Biomed Pharmacother* 2020, **123**:109666.
30. Ye Y, Zhang F, Chen Q, Huang Z, Li M: **LncRNA MALAT1 modified progression of clear cell kidney carcinoma (KIRC) by regulation of miR-194-5p/ACVR2B signaling**. *Mol Carcinog* 2019, **58**(2):279-292.
31. Candido J, Hagemann T: **Cancer-related inflammation**. *J Clin Immunol* 2013, **33 Suppl 1**:S79-84.
32. Swann JB, Smyth MJ: **Immune surveillance of tumors**. *J Clin Invest* 2007, **117**(5):1137-1146.
33. Thompson RH, Dong H, Lohse CM, Leibovich BC, Blute ML, Cheville JC, Kwon ED: **PD-1 is expressed by tumor-infiltrating immune cells and is associated with poor outcome for patients with renal cell carcinoma**. *Clin Cancer Res* 2007, **13**(6):1757-1761.
34. Yang H, Liang N, Wang M, Fei Y, Sun J, Li Z, Xu Y, Guo C, Cao Z, Li S *et al*: **Long noncoding RNA MALAT-1 is a novel inflammatory regulator in human systemic lupus erythematosus**. *Oncotarget* 2017, **8**(44):77400-77406.
35. Cao S, Wang Y, Li J, Lv M, Niu H, Tian Y: **Tumor-suppressive function of long noncoding RNA MALAT1 in glioma cells by suppressing miR-155 expression and activating FBXW7 function**. *Am J Cancer Res* 2016, **6**(11):2561-2574.
36. Haasch D, Chen YW, Reilly RM, Chiou XG, Koterski S, Smith ML, Kroeger P, McWeeny K, Halbert DN, Mollison KW *et al*: **T cell activation induces a noncoding RNA transcript sensitive to inhibition by immunosuppressant drugs and encoded by the proto-oncogene, BIC**. *Cell Immunol* 2002, **217**(1-2):78-86.
37. Singer J, Jensen-Jarolim E: **IgE-based Immunotherapy of Cancer -A Comparative Oncology Approach**. *J Carcinog Mutagen* 2014, **5**(3):1000176.
38. Casero RA, Jr., Marton LJ: **Targeting polyamine metabolism and function in cancer and other hyperproliferative diseases**. *Nat Rev Drug Discov* 2007, **6**(5):373-390.

39. Vliagoftis H, Boucher WS, Mak LL, Theoharides TC: **Inhibition of mast cell secretion by oxidation products of natural polyamines**. *Biochem Pharmacol* 1992, **43**(10):2237-2245.
40. Rohr-Udilova N, Klinglmuller F, Schulte-Hermann R, Stift J, Herac M, Salzmann M, Finotello F, Timelthaler G, Oberhuber G, Pinter M *et al*: **Deviations of the immune cell landscape between healthy liver and hepatocellular carcinoma**. *Sci Rep* 2018, **8**(1):6220.
41. Gu-Trantien C, Willard-Gallo K: **Tumor-infiltrating follicular helper T cells: The new kids on the block**. *Oncoimmunology* 2013, **2**(10):e26066.
42. Hosseini H, Obradovic MMS, Hoffmann M, Harper KL, Sosa MS, Werner-Klein M, Nanduri LK, Werno C, Ehrl C, Maneck M *et al*: **Early dissemination seeds metastasis in breast cancer**. *Nature* 2016, **540**(7634):552-558.
43. **The cancer genome atlas database (TCGA database).** https://portal.gdc.Cancer.gov/. Accessed 13 October 2020.

Figures

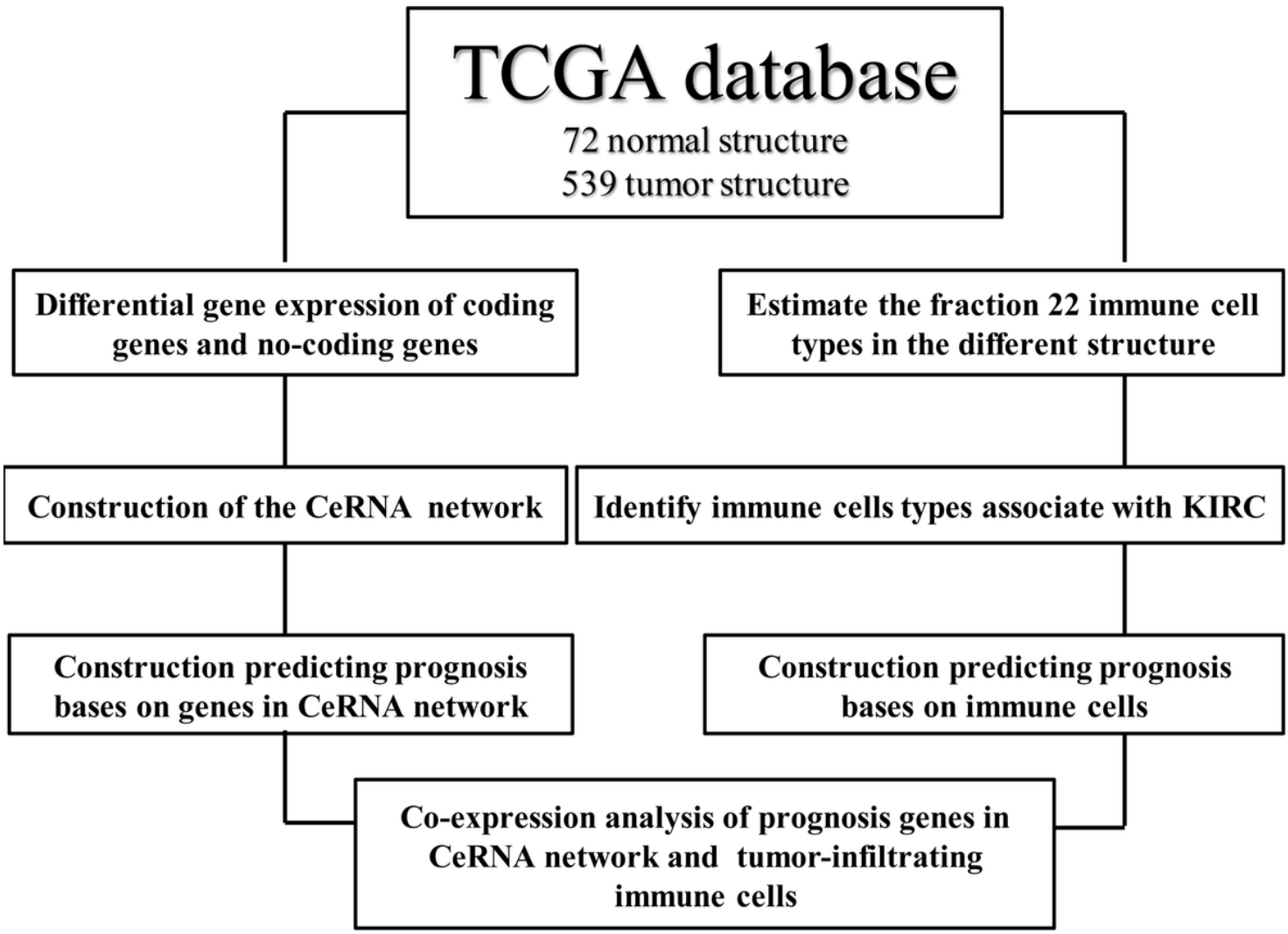

Figure 1

The Flowchart of the Analytical Process TCGA: The Cancer Genome Atlas.

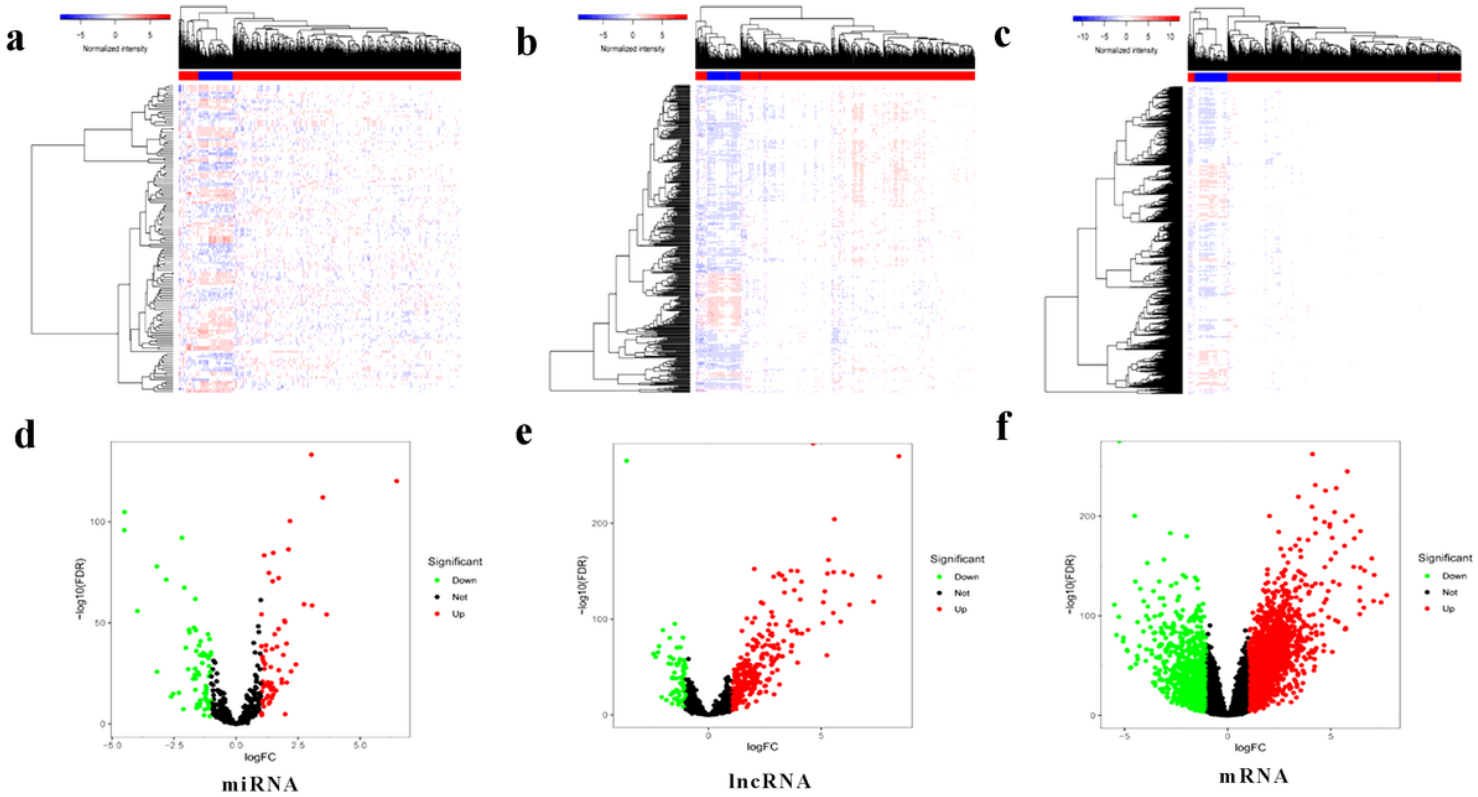

Figure 2

Identification of Differentially expressed Genes A: Heat map of differentially expressed mRNA. B: Heat map of differentially expressed lncRNA. C: Heat map of differentially expressed miRNA. D: Volcano map of differentially expressed mRNA. E: Volcano map of differentially expressed lncRNA. F: Volcano map of differentially expressed miRNA

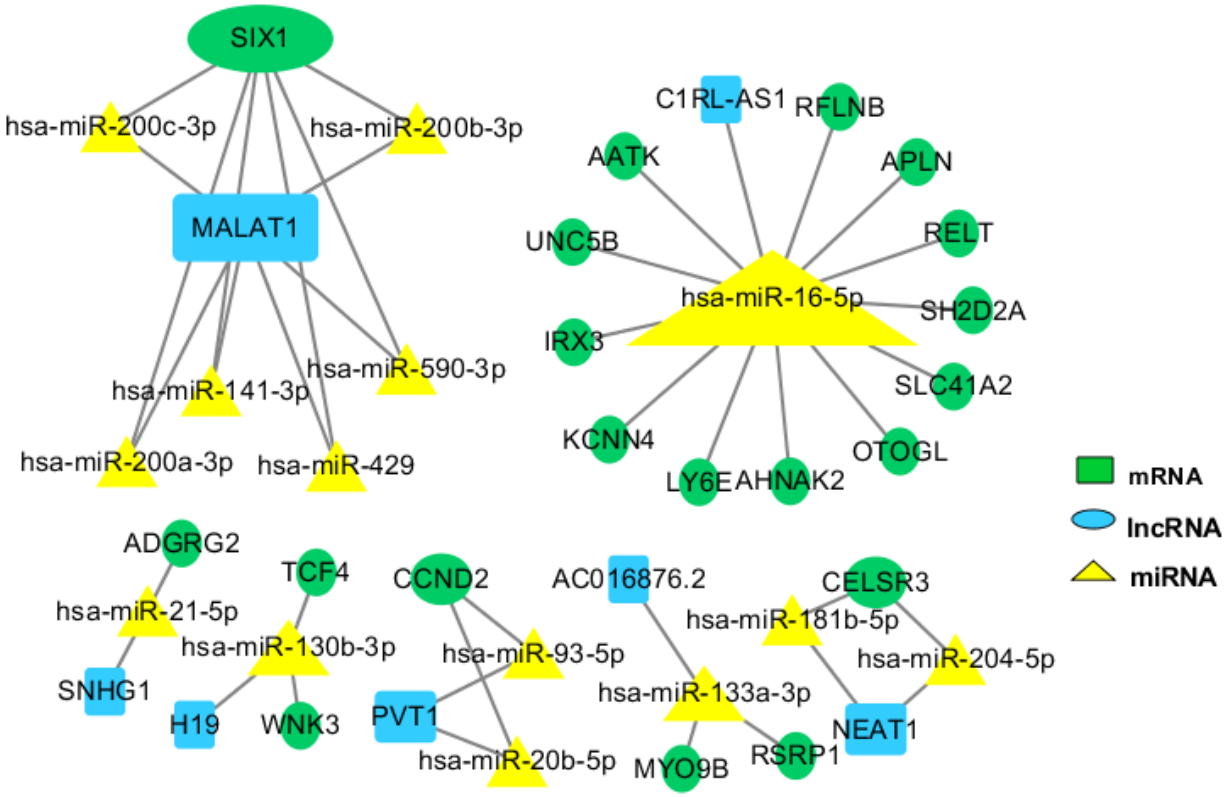

Figure 3

Construction of CeRNA Network The larger the width of each gene icon, the more nodes connected to the gene. Green: mRNA. Blue: lncRNA. Yellow: miRNA.

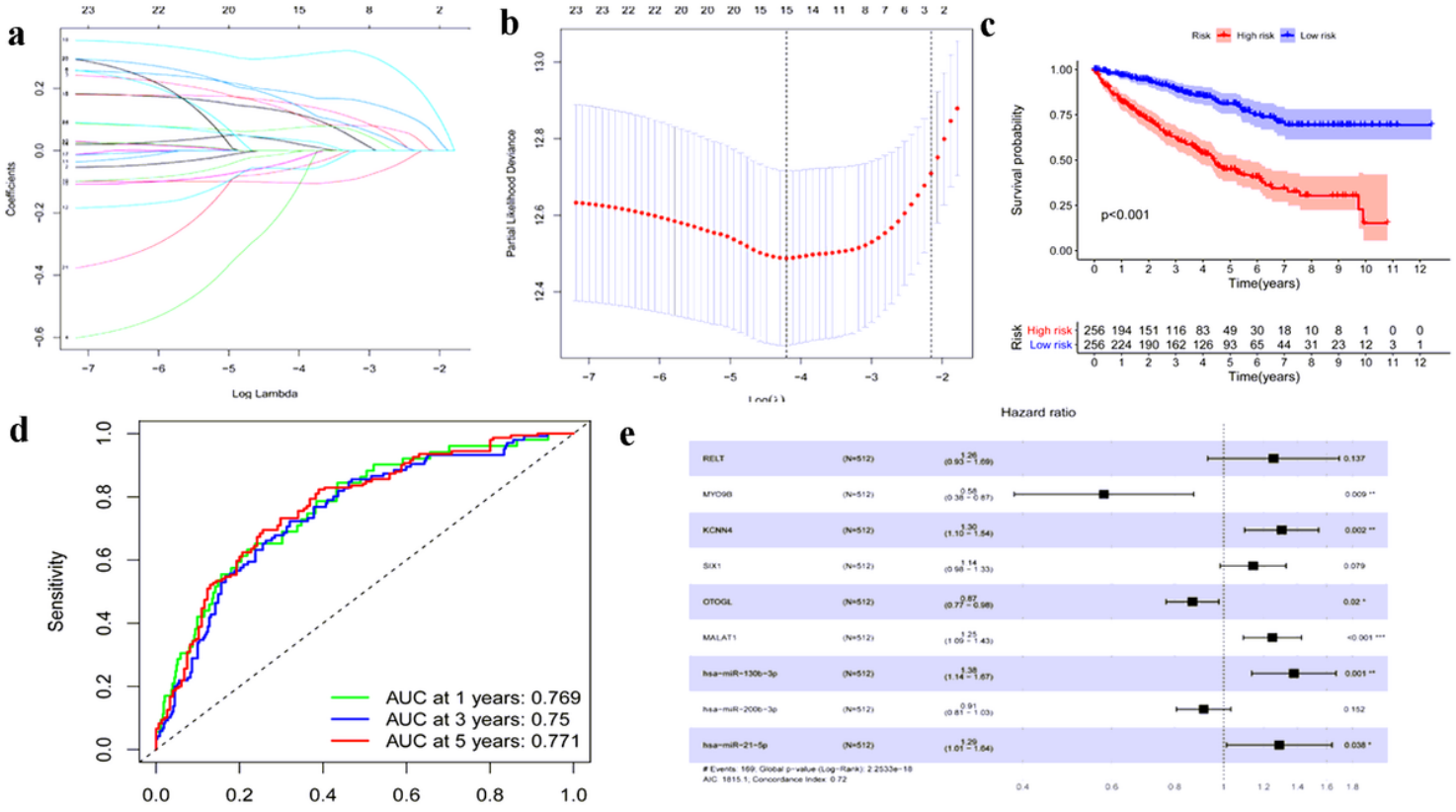

Figure 4

Construction of Risk Prognosis Model A, B: results of lasso regression analysis. C: model survival curve drawn by Kaplan-Meier method, Blue: low-risk Group, Red: high-risk group, P<0.001. D: ROC curve (the value of AUC represents the area under the curve). E: Multivariate Cox regression analysis, Hazard ratio>1 represents positive correlation, Hazard ratio<1 represents negative correlation.

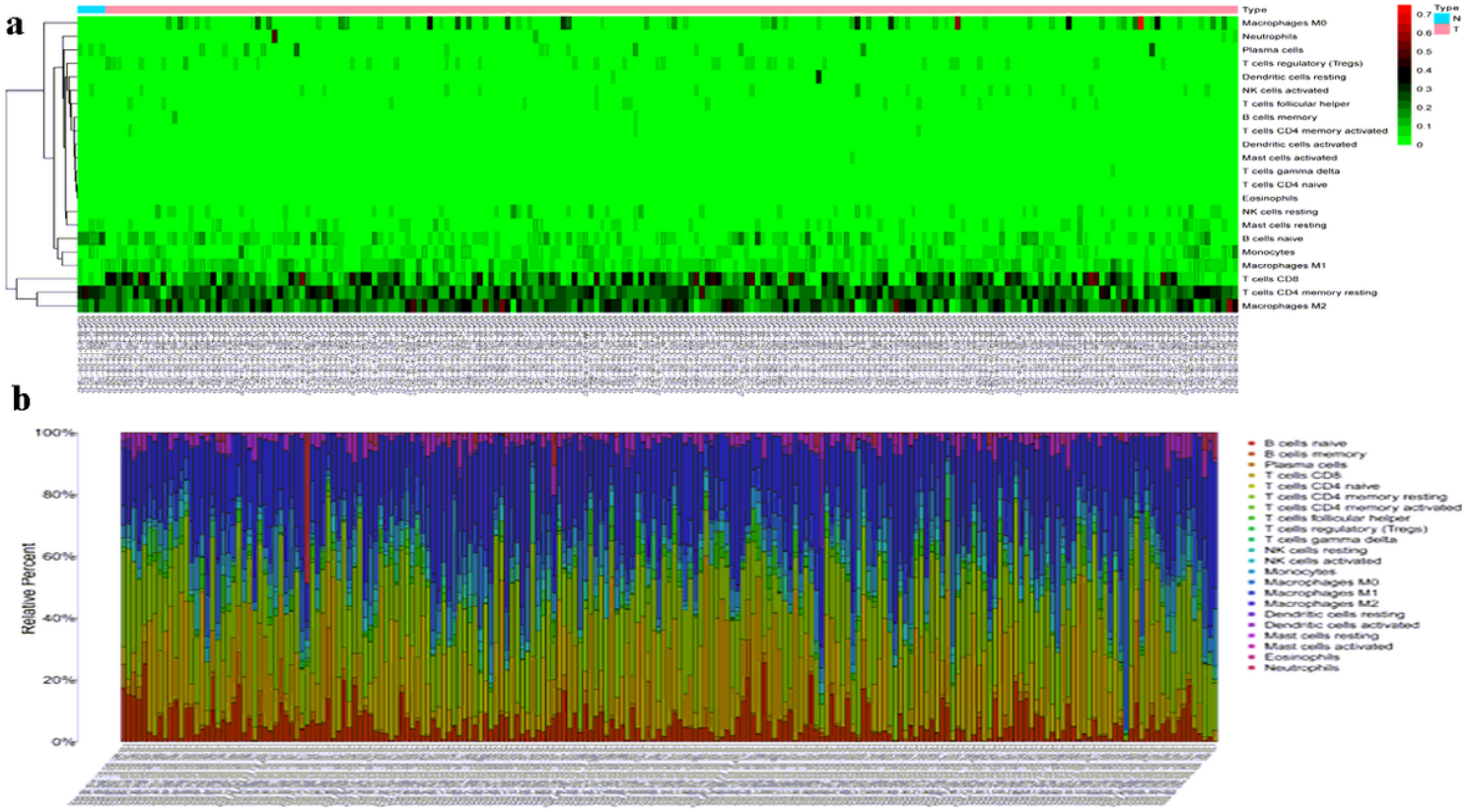

Figure 5

Identification of Differentially expressed Immune Cells A: The heat map of differential immune cells B: The histogram of differential immune cells.

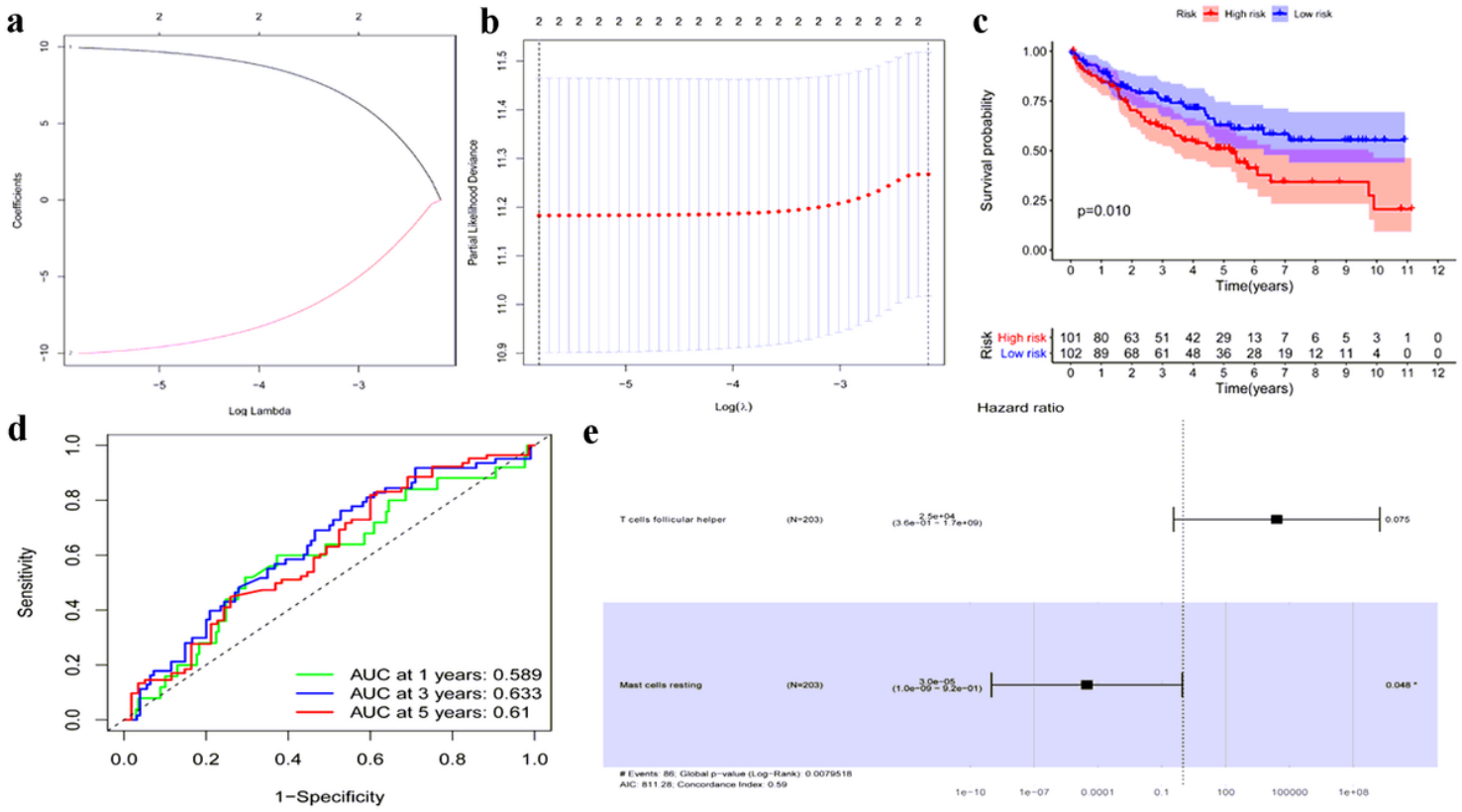

Figure 6

Construction of Risk Prognosis Model A, B: Results of lasso regression analysis. C: Survival curve drawn by Kaplan-Meier method, Blue: low-risk group, Red: high-risk group, P=0.01. D: ROC curve (the value of AUC represents the area under the curve). E: Multivariate Cox regression analysis, Hazard ratio>1 represents positive correlation, Hazard ratio<1 represents negative correlation.

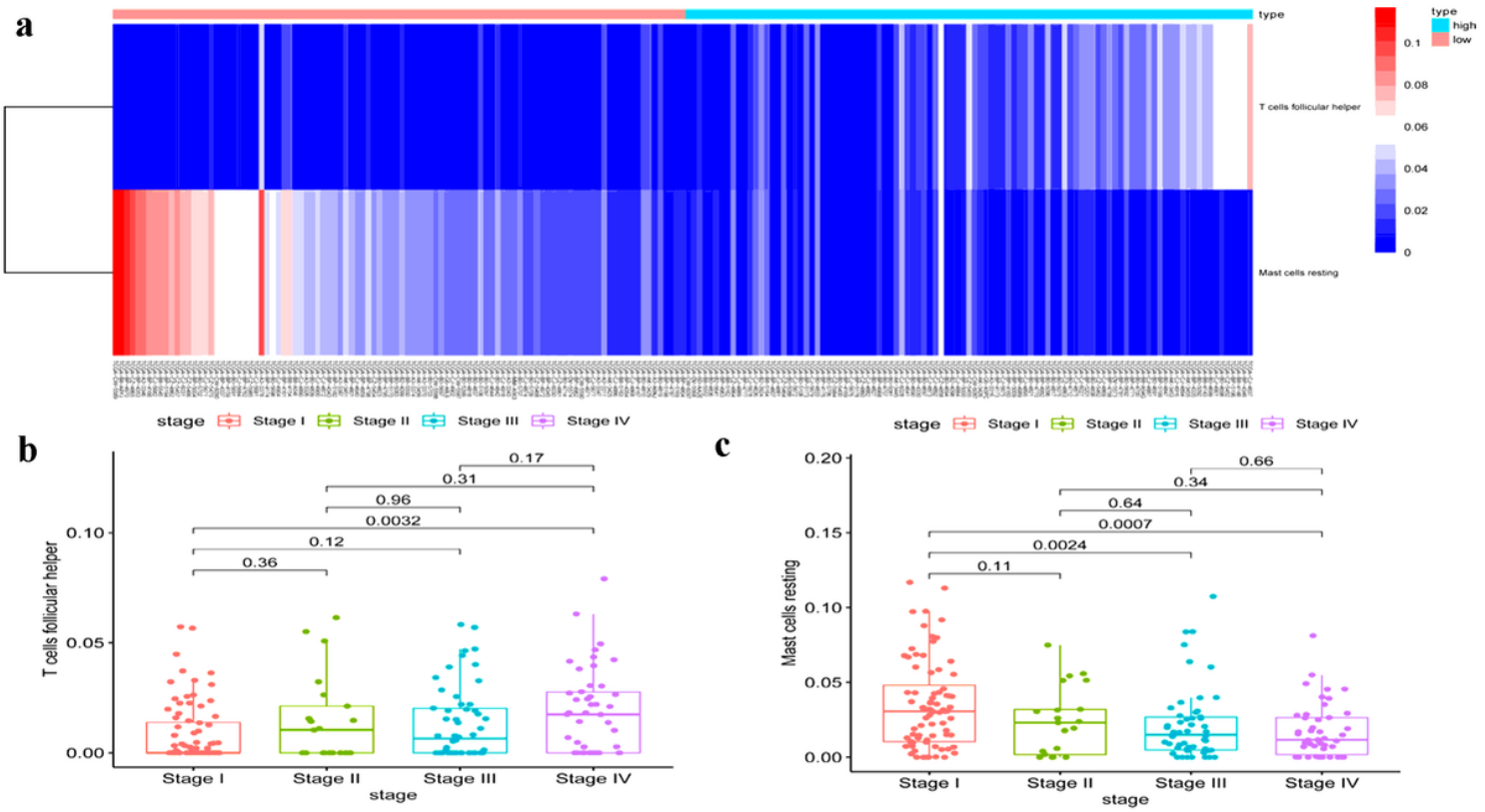

Figure 7

Expression Quantitative of Immune Cells in Different Stages of Clinical A: Heat map of the expression of risk immune cells in the low-risk group and the high-risk group. Pink: low-risk group, Green: high-risk group, Blue: low expression, Red: high expression. B: The expression quantitative of T cells follicular helper in different stages. C: The expression quantitative of Mast cells resting in different stages.

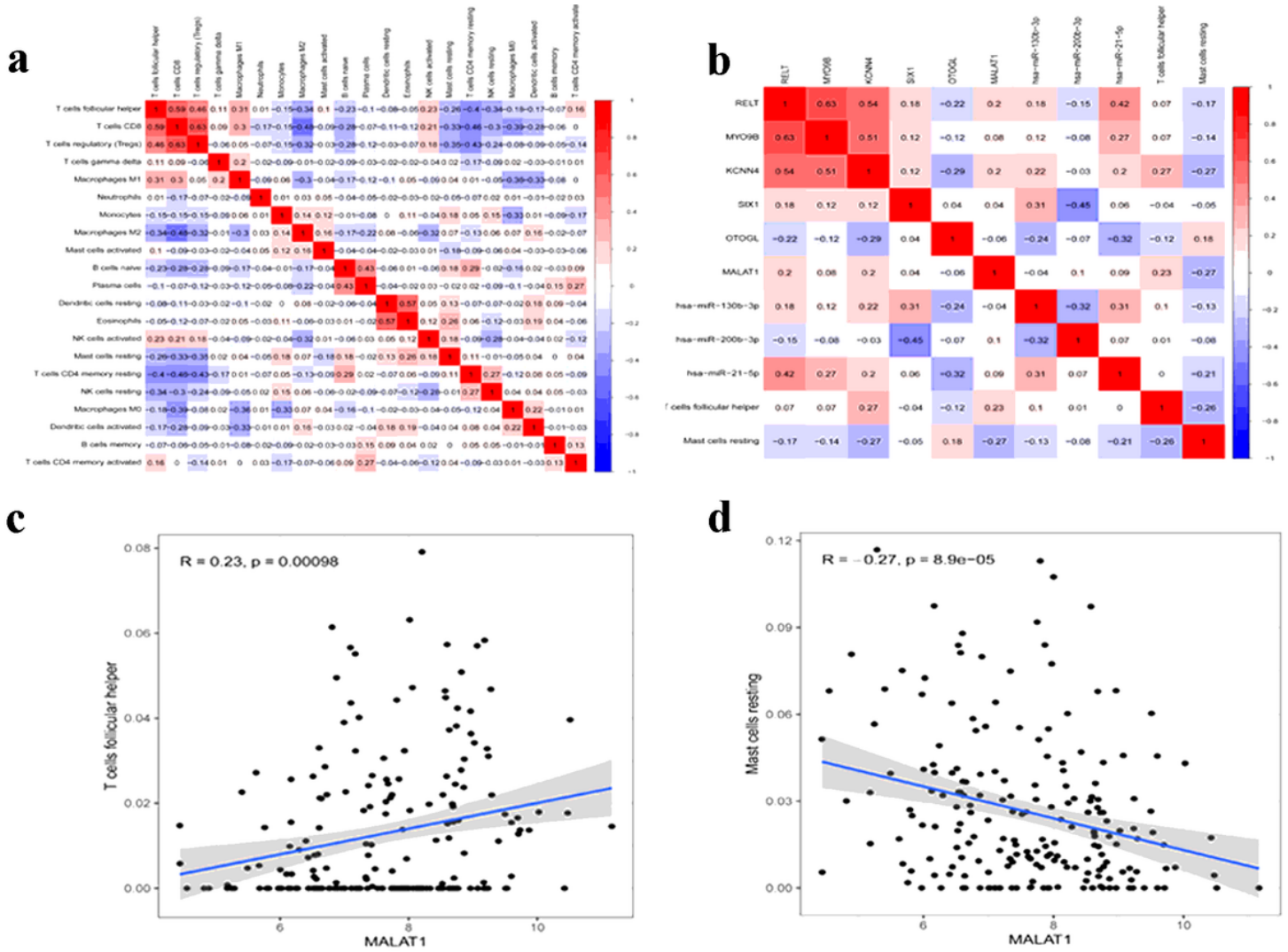

Figure 8

Co-expression Analysis A: Co-expression relationship diagram between immune cells. Red: positive correlation, Blue: negative correlation. B: Co-expression relationship diagram between immune cells and key genes in the CeRNA network. Red: positive correlation, Blue: Negative correlation. C: Correlation between lncRNA MALAT1 and Mast cells resting, P<0.001. D: Correlation between lncRNA MALAT1 and T cells follicular helper, P<0.001.

Supplementary Files

This is a list of supplementary files associated with this preprint. Click to download.

- Supplementarytable1.xls
- Supplementarytable2.xls
- Supplementarytable3.xls

- Supplementarytable4.xls
- Supplementarytable5.xls